



## Pharmaceutical Nanotechnology

## Formation of celecoxib nanoparticles from volatile microemulsions

Katrin Margulis-Goshen<sup>a</sup>, Ellina Kesselman<sup>b</sup>, Dganit Danino<sup>b,c</sup>, Shlomo Magdassi<sup>a,\*</sup><sup>a</sup> Casali Institute of Applied Chemistry, Institute of Chemistry, The Hebrew University of Jerusalem, Jerusalem, Israel<sup>b</sup> Department of Biotechnology and Food Engineering, Technion Israel Institute of Technology, Haifa, Israel<sup>c</sup> Russell Berrie Nanotechnology Institute, Technion Israel Institute of Technology, Haifa, Israel

## ARTICLE INFO

## Article history:

Received 31 January 2010

Received in revised form 4 April 2010

Accepted 10 April 2010

Available online 18 April 2010

## Keywords:

Organic nanoparticles

Microemulsion

Evaporation

Poorly soluble drug

Celecoxib

## ABSTRACT

A new composition of a fully water-dilutable microemulsion system stabilized by natural surfactants is presented as a template for preparation of celecoxib nanoparticles. Nanoparticles are obtained as a dry powder upon rapid conversion of microemulsion droplets with dissolved celecoxib into nanoparticles, followed by evaporation of all the liquid in a spray dryer. The resultant powder is easily re-dispersible in water to form a clear, transparent dispersion. The celecoxib nanoparticles are amorphous and their average size in the dispersion is 17 nm, in agreement with cryo-TEM results and concentration measurements after filtration. As a result of the nanometric size and amorphous state, about 10-fold increase in dissolution of the powder was obtained, compared to that for particulate celecoxib in the presence of surfactants.

© 2010 Elsevier B.V. All rights reserved.

## 1. Introduction

Low aqueous solubility of an active pharmaceutical ingredient presents a major challenge for the pharmaceutical industry when developing dosage forms for drugs belonging to classes 2 and 4 of the Biopharmaceutical Classification System.

It is well known that bioavailability of poorly water-soluble drugs for oral delivery may be significantly improved by reducing the drug particle size to the nanometric range (Horn and Rieger, 2001). In addition to greater dissolution rate and saturation solubility (Noyes and Whitney, 1897; Knapp, 1921; Rabinow, 2004), it was reported that nanoparticles exhibit greater bioadhesiveness compared to particulate drugs due to their large surface area (Keck and Muller, 2006).

Nanoparticles of poorly soluble drugs can be obtained by a variety of methods, including wet/dry milling (Bushrab and Müller, 2003; Merisko-Liversidge and Liversidge, 2008), controlled precipitation from solution (Chen et al., 2002, 2006; Matteucci et al., 2006, 2007), flash nanoprecipitation (Zhu et al., 2007), supercritical solution expansion (Turk et al., 2002; Perrut et al., 2005), spray freezing into liquid/spray freeze drying (Hu et al., 2004; Niwa et al., 2009), and solvent evaporation from emulsions (Desgouilles et al., 2003).

Solvent evaporation from oil-in-water emulsion is a very common method for drug nanoparticle preparation. By this method, a drug is dissolved in a volatile water-immiscible solvent and this

solution is emulsified in water using high shear equipment, such as high-pressure homogenizers. Eventually, the organic solvent is removed and drug particles are formed in the same size range as the emulsion droplets.

Small droplet size can be achieved by using microemulsions, which are spontaneously formed without any special equipment and are thermodynamically stable. The ease and the low cost of the preparation process make them very attractive confined structures for preparation of nanoparticles.

So far, most of the publications regarding formation of drug nanoparticles from microemulsions have been based on precipitation of the drug. For example, nanoparticles of retinol were prepared by precipitation in water-in-oil microemulsion (Debuigne et al., 2000; Destree et al., 2006, 2007), and nanoparticles of griseofulvin were obtained by the solvent diffusion technique (Trotta et al., 2003).

Only recently has solvent evaporation from oil-in-water microemulsions been applied for obtaining nanoparticles of several hydrophobic materials (Magdassi et al., 2007; Margulis-Goshen et al., 2010). For example, simvastatin nanoparticles with enhanced dissolution were formed by lyophilization of an oil-in-water microemulsion (Margulis-Goshen and Magdassi, 2009).

In this report we present a simple method for preparation of a water-dispersible powder that contains nanoparticles of a poorly soluble drug, celecoxib, while using only natural surfactants. By this method the drug is dissolved in a hydrophobic solvent, which has an evaporation rate greater than that of water. Natural surfactants, volatile cosurfactant, and water are added to the drug solution to spontaneously form a microemulsion. The microemul-

\* Corresponding author. Tel.: +972 2 658 4967; fax: +972 2 658 4350.  
E-mail address: [magdassi@cc.huji.ac.il](mailto:magdassi@cc.huji.ac.il) (S. Magdassi).

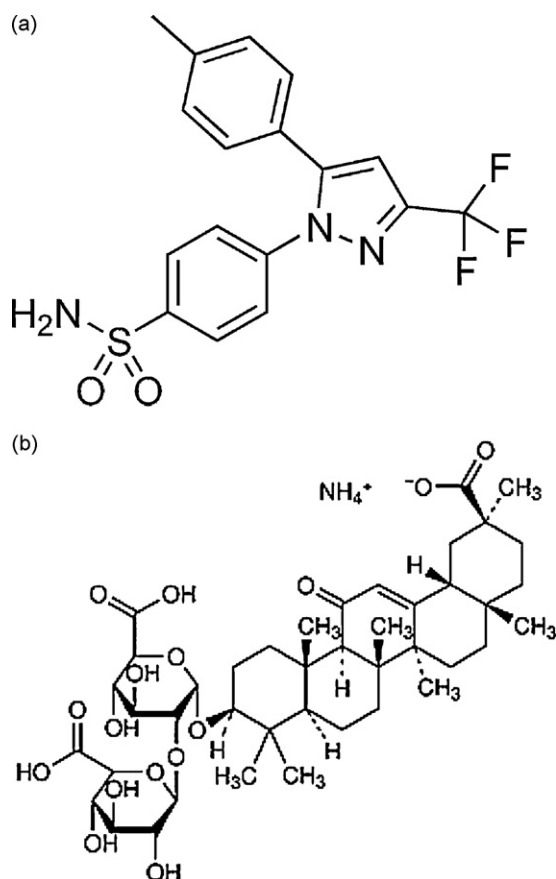


Fig. 1. (a) Celecoxib structure. (b) Ammonium glycyrrhizinate structure.

sion is directly converted into a dry powder by spray drying. This process removes all the liquids (water and organic) at once, thus the nanodroplets of the drug solution convert into nanoparticles of the drug, together with all the non-volatile components of the microemulsion.

The celecoxib that is used here as a model for a water-insoluble drug (Fig. 1a), is a specific cyclooxygenase-2 (COX-2) inhibitor that is successfully used for treating arthritis (Detrembleur et al., 2005; Kivitz et al., 2007; Yelland et al., 2007), pain alleviating (Lu et al., 2006), treating familial adenomatous polyposis and preventing colorectal adenocarcinomas (Dannenberg and Subbaramaiah, 2003; Bertagnolli et al., 2006; Auman et al., 2008; Chan et al., 2009).

The aqueous solubility of celecoxib is 3–7 µg/ml at pH 7 and 40 °C. The absolute bioavailability after oral administration of the solid dosage form of celecoxib in dogs is 22–40% (Paulson et al., 2001). It is a lipophilic compound ( $\log P=3.5$ ) (Shono et al., 2009) and has been proven to belong to the class 2 division of the Biopharmaceutical Classification System – poorly soluble and highly permeable drugs (Paulson et al., 2001). It is generally accepted that compounds with low solubility and high permeability through biological membranes will show dissolution rate-limited absorption *in vivo*. Therefore, improving the solubility of such a drug is expected to enhance bioavailability and hence therapeutic potency.

The goal of the present research was to form nanoparticles with pharmaceutically acceptable, GRAS listed (generally regarded as safe), natural amphiphiles.

To achieve this goal, at the first stage, microemulsion stabilized by pharmaceutically acceptable surfactants had to be formed. Soybean phosphatidylcholine (SbPC) is a widely used surfactant of natural origin, a known food additive, and is safe for intravenous and oral drug delivery routes. This makes it an excellent candi-

date for our system. However, phosphatidylcholine alone does not form microemulsions. A possible way to obtain an oil-in-water microemulsion and preserve the initial form of the nanoparticles during the evaporation process is to partially replace SbPC with another amphiphile, preferably a more hydrophilic one. As shown by Trotta et al. (2003), dipotassium glycyrrhizinate or sodium taurocholate enabled formation of microemulsions that were fully dilutable with the aqueous phase (solution of hydrophilic amphiphile in water), but not with water alone.

In this study we used ammonium glycyrrhizinate (AG) as the second amphiphile, which is slightly soluble in water (Fig. 1b). Glycyrrhizic acid is a natural triterpenoid saponin extracted from licorice root. Glycyrrhizic acid and its salts can act as emulsifiers but also possess hepatoprotective, anti-inflammatory, anti-allergic, anti-viral, antidepressant, and gastric mucosal protective properties (Dhingra and Sharma, 2005; Archakov et al., 2007; Oh et al., 2009). They are listed as GRAS food additives and are approved by the FDA for incorporation into oral pharmaceutical preparations. They have been utilized as surface-active agents, lipid bilayer fluidizers for preparation of deformable liposomes, and as natural active ingredients exhibiting anti-inflammatory characteristics (Trotta et al., 2003, 2004; Paolino et al., 2005; Lin et al., 2008).

It was expected that once a microemulsion with a volatile oil phase is obtained, rapid evaporation of all the liquids would lead to a powder composed of nanometric particles of the celecoxib and surfactants that are FDA and GRAS approved.

## 2. Materials and methods

### 2.1. Materials

Celecoxib was a gift of Teva Pharmaceutical Industries (Israel), n-butyl acetate, sec-butyl alcohol and ammonium glycyrrhizinate were obtained from Sigma-Aldrich (Israel), Epikuron 200 lecithin with at least 92% soybean phosphatidylcholine was supplied by Cargill (Germany). HPLC grade water was obtained from Bio-Lab (Israel) and HPLC grade methanol was obtained from Merck (Israel).

### 2.2. Microemulsion preparation

Concentrates of n-butyl acetate (nBuAc) and surfactant mixtures (sec-butyl alcohol (secBuOH), AG and SbPC) were prepared at various ratios and allowed to equilibrate at 25 °C for 24 h. Afterwards, the concentrates were gradually diluted with water, at intervals of 10 wt% water. The resulting compositions were equilibrated for 24 h at 25 °C. Only compositions that remained transparent and homogeneous after this period of time were attributed to the monophasic area in the phase diagram. The phase diagram was prepared for microemulsions without celecoxib.

### 2.3. Electrical conductivity measurements

Electrical conductivity measurements of the microemulsion were performed at 25 °C using an Oyster conductivity meter (Extech, USA). In order to increase the electrical conductivity of the aqueous phase, it was replaced with 0.01 M NaCl aqueous solution.

### 2.4. Cryogenic-transmission electron microscopy (cryo-TEM)

Drug-loaded microemulsion and nanoparticles after dispersing the powder in water were evaluated by cryo-TEM. A 7 µl drop of the solution was placed on a perforated carbon film supported on a TEM copper grid, held by tweezers inside the controlled-environment vitrification system (Bellare et al., 1988). It was then blotted with a piece of filter paper, resulting in the formation of thin sample films

within the micropores in the carbon-coated lacy polymer layer supported on the grid. The specimen was then plunged into a reservoir of liquid ethane and cooled by liquid nitrogen, to ensure its vitrification and to prevent ice crystal formation. The vitrified specimen was transferred under liquid nitrogen to a Gatan 626 cryogenic sample holder, cooled to  $-170^{\circ}\text{C}$ . All samples were studied under low-dose conditions in an FEI T<sup>12</sup> G2 TEM, operating at 120 kV. Images were recorded on a Gatan US1000 high-resolution cooled CCD camera and processed with the DigitalMicrograph version 3.4 software. The ramp-shaped optical density gradients in the background were digitally corrected (Danino et al., 2001; Cui et al., 2007).

## 2.5. Image analysis of cryo-TEM images

Digital cryo-TEM images of celecoxib nanoparticles dispersed in water were analyzed using software developed under Matlab (Mathworks, Natick, MA, USA). The images were preprocessed against the background noise (despackled) as well as compensated for the underfocused acquisition method (deconvolution). The images were then segmented to identify the individual particles and underwent a limited watershed split to separate overlapping objects. Calibrated measurements of area, mean diameter, feret diameter, and roundness were extracted for each object and filtered to eliminate artifacts (filter parameters: area > 100 sq./nm, aspect < 3, roundness < 3.5).

## 2.6. Converting microemulsion to nanoparticles

Drug-loaded microemulsions were spray dried by a Mini-laboratory Spray Dryer B-290 equipped with inert loop dehumidifier B-296 (Buchi, Flawil, Switzerland). Process conditions were: air inlet temperature  $110^{\circ}\text{C}$ , drying chamber (outlet) temperature  $60^{\circ}\text{C}$ , liquid introduction rate 5 ml/min, spray flow rate 414 normlitter/h, aspirator rate 35 m<sup>3</sup>/h, nitrogen pressure 6 atmospheres.

## 2.7. X-ray diffraction (XRD)

X-ray powder diffraction measurements were performed by the D8 Advance diffractometer (Bruker AXS, Karlsruhe, Germany) with a goniometer radius 217.5 mm, Göbel Mirror parallel-beam optics,  $2^{\circ}$  Sollers slits and 0.2 mm receiving slit. Standard sample holders were carefully filled with the samples. The specimen weight was approximately 0.5 g. XRD patterns within the range of  $5^{\circ}$  to  $35^{\circ} 2\theta$  were recorded at room temperature using CuK $\alpha$  radiation ( $\lambda = 1.5418 \text{ \AA}$ ) with following measurement conditions: tube voltage of 40 kV, tube current of 40 mA, step-scan mode with a step size of  $0.02^{\circ} 2\theta$ , and counting time of 1 s/step.

## 2.8. Powder dispersion in water

Powder obtained at the end of the spray drying process was dispersed (0.5–1 wt%) in deionized water. The samples were vortexed for 1 min and magnetically stirred at room temperature for 5 min. This procedure for dispersing the powder was performed in order to have a reproducible procedure, although simple manual shaking of the dispersion for 1–2 min was sufficient to obtain an optically clear system.

## 2.9. Particle size distribution measurements

The size distribution of particles after dispersion in water was measured at room temperature by dynamic light scattering by a Nano-ZS Zetasizer (Malvern, UK). The instrument is equipped with 633 nm laser, and the light scattering is detected at  $173^{\circ}$  by a back

scattering technology (NIBS, Non-Invasive Back-Scatter). Measurements were performed in the triplicate.

## 2.10. Zeta ( $\zeta$ ) potential measurement

$\zeta$  Potential measurements were performed at  $25^{\circ}\text{C}$  using a Zeta-master (Malvern, UK). The voltage in the measurement cell was 150 V.  $\zeta$  Potential was measured in triplicate for powders that were dispersed in 10 mM NaCl. To evaluate  $\zeta$  potential at normal physiological blood pH, the pH of 0.5 wt% dispersion of powder in 10 mM NaCl was adjusted to 7.4 by diluted NaOH solution. The ionic strength was kept constant for all samples.

## 2.11. Celecoxib concentration in nanoparticles

The concentration of celecoxib in the nanoparticles was determined after filtration of powders dispersed (0.5 wt%) in water (0.45  $\mu\text{m}$  filter–Millex® VV-PVDF filter produced by Millipore, Ireland). The celecoxib concentration in the filtrate was determined by an RP-HPLC HP1050 equipped with an RP8 column (Hewlett Packard, USA). Mobile phase was methanol: water (75:25, v/v) (Baboota et al., 2007) and its flow rate was 1 ml/min. Prior to injection the samples were diluted in methanol:water solution (50:50, v/v). The UV detection was performed at 250 nm, and the response was linear between 0.001 and 0.05 wt%. All measurements were performed in triplicate.

## 2.12. Determination of fraction of celecoxib dissolved

To separate between dissolved and nanometrically dispersed celecoxib, 0.5 wt% powder dispersion in water was ultrafiltered (Centrifuge CN-2200 MRC, Israel) for 10 min at 4000 rpm using four 300,000 D filtration tubes (VS0241 Viva spin tubes, Sartorius Stedim Biotech, Germany). Celecoxib concentration in the filtrate was detected by HPLC as above and was regarded as concentration of dissolved celecoxib.

## 2.13. Control experiments

Two control experiments were performed to validate the necessity of the microemulsion preparation route: solubilization of celecoxib within micelles at room and elevated temperatures, and the attempt to form a solid solution instead of nanoparticles. Possible solubilization was evaluated by dispersing the raw material (large crystals) in water, with two surfactants at concentrations similar to those of components in 0.5% water dispersion of powder (celecoxib 0.0555 wt%, ammonium glycyrrhizinate 0.222 wt%, soybean phosphatidylcholine 0.222 wt%, and water 99.5 wt%). The mixture was stirred for 6 h at various temperatures (room temperature, 40 and  $60^{\circ}\text{C}$ ) followed by immediate filtration and measurements of the concentration of dissolved/solubilized celecoxib by HPLC. The possibility of solid solution formation was evaluated by mixing celecoxib and the surfactants in a solution of nBuAc/secBuOH (0.175/0.1) at concentrations similar to that of the initial microemulsion composition (celecoxib 2.5 wt%, ammonium glycyrrhizinate 10 wt%, soybean phosphatidylcholine 10 wt%), followed by evaporation of the solvents by heating. The resultant solid was dispersed in water at 0.5 wt%, and the celecoxib concentration was determined as in the procedure for measuring celecoxib concentration in nanoparticles (described above).

## 2.14. Dissolution test

Dissolution test was performed using a Caleva dissolution bath (USP Apparatus II bath, 1 L beakers). Dissolution medium was USP 26 simulated intestinal fluid TS (without pancreatin, pH



6.8, (Steippler et al., 2004)). The dissolution experiments were conducted at  $37 \pm 0.5^\circ\text{C}$  at a paddle rate of 100 rpm for 30 min. Sampling was performed after 1, 2, 5, 10, 15, and 30 min according to the pharmacopoeia sampling process requirements (USP30-NF25). Withdrawn liquid was replaced with dissolution medium. Detection of celecoxib concentration was performed by HPLC (samples filtered through a  $0.45\ \mu\text{m}$  filter).

### 2.15. Comparison to a conventional particulate drug

A comparative dissolution test was conducted for the obtained nanopowder (0.36 wt%, equal to 0.04 wt% celecoxib), celecoxib raw material (0.04 wt%), and celecoxib bulk powder with the two surfactants (celecoxib 0.04 wt%, ammonium glycyrrhizinate 0.16 wt%, soybean phosphatidylcholine 0.16 wt%).

## 3. Results and discussion

### 3.1. Phase diagrams for microemulsion systems

The phase diagram was constructed at  $25^\circ\text{C}$  for systems containing SbPC, AG, and secBuOH in equal weight proportions as the “surfactant-cosurfactant” component, and n-butyl acetate as the oil phase. Sec-butyl alcohol was selected as the short chain alcohol that would further reduce the critical packing parameter and the rigidity of phosphatidylcholine interfacial film allowing it the sufficient flexibility required to form microemulsions (De Gennes and Taupin, 1982). secBuOH has an evaporation rate similar to that of n-butyl acetate and its aqueous solubility is low compared to the shorter chain alcohols. Due to those properties it is expected that secBuOH will be mostly located at the droplet interface rather than at the aqueous phase of the microemulsion. During the evaporation process this alcohol should evaporate at a rate similar to that of nBuAc, instantly forming oil-free nanoparticles. The phase diagram is shown in Fig. 2. As can be clearly seen, the above components indeed led to formation of microemulsions, while an isotropic phase (microemulsion) is obtained at all water fractions.

As shown, microemulsions that are located along dilution line 4:6 oil to surfactant weight ratio are fully dilutable with water. The microemulsion composition chosen for drug loading (labeled with an asterisk in the phase diagram) is 20 wt% nBuAc, 10 wt% secBuOH,

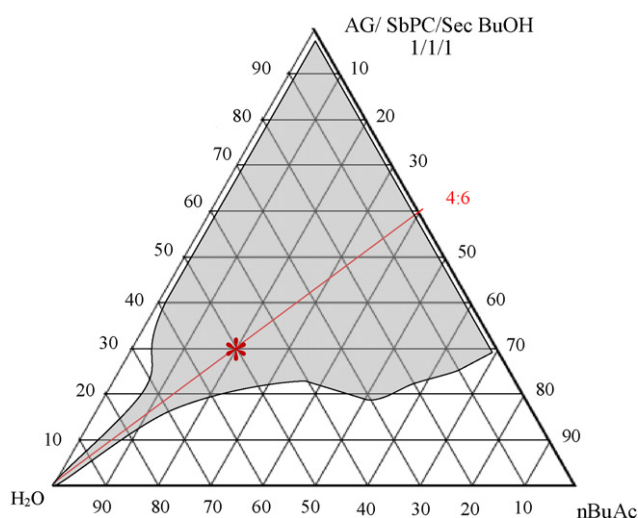


**Fig. 2.** Phase diagram describing the formation of nBuAc-water microemulsions stabilized by AG/SbPC/Sec BuOH surfactants in weight fractions of 1/1/1. Shadowed area represents microemulsion formation region.

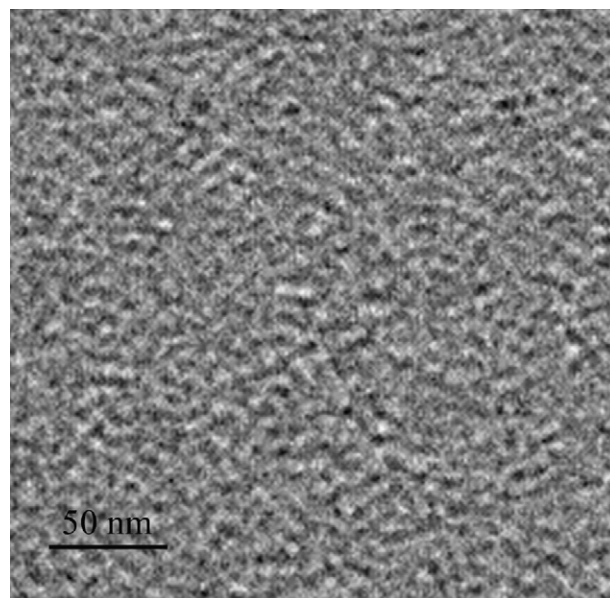


**Fig. 3.** Cryo-TEM picture of celecoxib-loaded microemulsion containing 2.5 wt% celecoxib, 17.5 wt% organic solvent, 30 wt% surfactant mixture, and 50 wt% water.

10 wt% SbPC, 10 wt% AG, and 50 wt% water, enabling a sufficient amount of drug to be present while dissolved in nBuAc.

### 3.2. Microemulsion characterization by electrical conductivity

In order to characterize the inner structure of this microemulsion, its electrical conductivity was measured and compared to the electrical conductivity of the oil and aqueous phase components. Electrical conductivity of the microemulsion was  $2.8 \pm 0.2\ \text{mS/cm}$  compared to  $2\ \mu\text{S/cm}$  for pure nBuAc and  $2.3\ \mu\text{S/cm}$  for secBuOH. The electrical conductivity of the dispersion of SbPC and AG in 10 mM NaCl solution (aqueous phase) was  $2.5 \pm 0.1\ \text{mS/cm}$ . Since the electrical conductivity of the microemulsion is about three orders of magnitude greater than that of the organic solvents and similar to that of the aqueous phase, it can be concluded that the microemulsion chosen for the nanoparticle preparation is oil-in-water type.

### 3.3. Loading the microemulsion with the drug

The chosen microemulsion composition was loaded with celecoxib by dissolving it in nBuAc prior to the formation of the microemulsion (final celecoxib concentration in the microemulsion is 2.5 wt%).

This drug-loaded microemulsion was imaged by cryo-TEM revealing the presence of discrete droplets as expected from oil-in-water microemulsion (Fig. 3). It can be seen from the image that the oil domains have a mean diameter of a few nanometers.

### 3.4. Nanoparticle formation and characterization

The drug-loaded microemulsion was spray dried and yielded a dry, free-flowing powder. Celecoxib concentration in this powder was 11.1%. XRD measurements performed on this powder indicated that celecoxib is present as an amorphous form, since no peaks of crystalline celecoxib were detected in diffraction patterns of the powder (Fig. 4). The drug remained in its amorphous form when the powder was stored at room temperature for at least 3 months.

It was found that this powder was easily dispersible (1 wt%) in water forming a transparent dispersion, as could be expected from

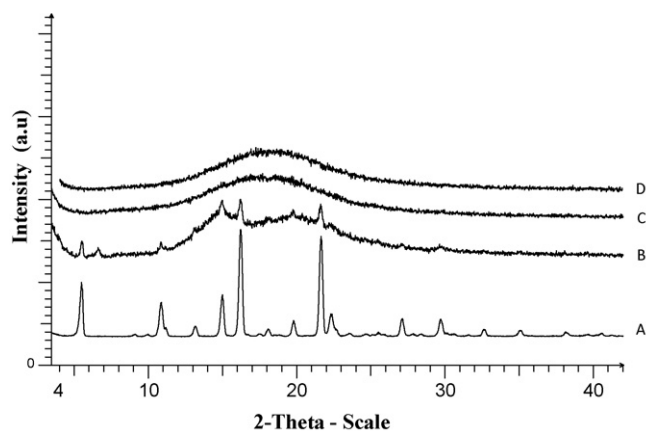


**Fig. 4.** X-ray diffraction patterns for crystalline celecoxib (A), mechanical mixture of powder components (B), freshly prepared nanopowder (C), nanopowder stored at room temperature for 3 months (D).

very small particles. The average particle size in this dispersion as measured by DLS was  $16.7 \pm 0.7$  nm. A typical DLS measurement of particle size distribution in this dispersion is shown in Fig. 5a.

The dispersion was also observed by cryo-TEM and its typical image is presented in Fig. 5b. Image analysis result of this cryo-TEM image indicates that the mean diameter of the particles is  $15.8 \pm 4.2$  nm.

In order to verify that the DLS measurements and Cryo-TEM observations are indeed related to the drug nanoparticles and not to particles of AG/SbPC without the drug (if the drug is completely dissolved), the following control experiment was conducted: 0.5 wt% powder dispersion in water was ultrafiltered (300 kDa cutoff) and celecoxib concentration in the filtrate was measured. It was found that  $21 \pm 4$  wt% of celecoxib passed this filter, indicating that the concentration of dissolved celecoxib is about 35 times higher than predicted by its literature solubility value. However, the majority of celecoxib is present as nanoparticles, which were measured by DLS and cryo-TEM.

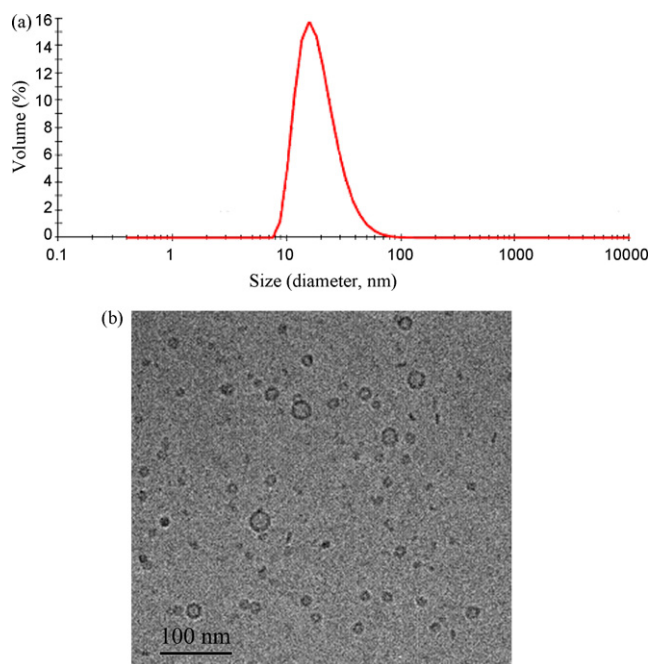


**Fig. 5.** (a) Typical DLS measurement of particle size distribution in nanodispersion. (b) Cryo-TEM image of 1 wt% powder dispersed in water.

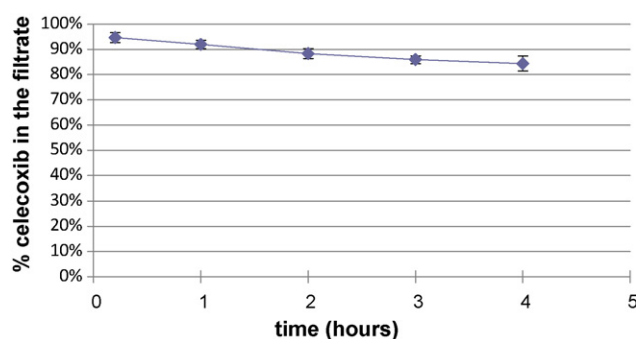


**Fig. 6.** Fraction of celecoxib found in particles smaller than 450 nm in aqueous dispersion at various time intervals after the re-dispersion.

It can be seen that the particle size in the nanodispersion is larger than the droplet size in the drug-loaded microemulsion. Growth of particles formed from water-in-oil microemulsion droplets was previously explained using crystallization models (Destree et al., 2007). A probable explanation for the larger size of the amorphous particles in our system is the possible coalescence of microemulsion droplets at some stage of the evaporation process. Although the evaporation rates of the bulk organic components (nBuAc/secBuOH) are much higher than that of pure water, it is well known that upon emulsification the evaporation rate of the dispersed phase might be retarded (Clint et al., 1999; Aranberri et al., 2002). Since solvent evaporation by spray drying is rapid, we expect that the microemulsion preserves its initial structure during the drying. However, we cannot rule out the possible collapse of the structure at the last stage of the process. Thus, particles larger than the initial droplet size may eventually be obtained.

Cryo-TEM images also revealed the presence of elongated nanometric structures, which resemble bilayer fragments. This observation is in agreement with a model proposed by Yoshioka et al. (1989), suggesting that glycyrrhizin is capable of breaking phospholipid membrane into small, ordered fragments.

For quantitative determination of the percentage of the drug that is present as nanoparticles, 0.5 wt% of the powder was dispersed in water and the resultant dispersion filtered through a  $0.45 \mu\text{m}$  filter. From measurements of celecoxib concentration in the filtrate it was found that about 95 wt% of the dispersed celecoxib is present in particles smaller than  $0.45 \mu\text{m}$  in diameter. It should be noted that there is probably an increase in the solubility of celecoxib due to its presence in the amorphous state, but such an increase cannot explain the presence of 95 wt% celecoxib in the filtrate. It was estimated by Gupta et al. (2004) that the solubility of amorphous celecoxib is only about 1.3 times higher than of that of the crystalline form. In this experiment, if we assume that all the celecoxib in the filtrate is dissolved, a 100-fold increase in solubility is achieved, which is impossible only in view of its amorphous state. Therefore, it can be concluded that most of the celecoxib is present as nanoparticles which are stabilized by adsorbed surfactants or dissolved due to the nanometric dimension of the particles. As shown in Section 3.5, some of the celecoxib is solubilized within the micelles of the surfactants.

The stability of the nanoparticles in the dispersion was evaluated by measuring the celecoxib concentration in the filtrate at various time intervals (Fig. 6). As seen, the percentage of drug that is present as particles smaller than 450 nm slightly decreases with time. When the dispersion is observed by light microscopy with and without polarized light, after 4 h very few small crystals ( $1\text{--}2 \mu\text{m}$ ) could be detected. However, 4 h after dispersion of the powder in water more than 85 wt% of celecoxib is still present as nanoparticles, and that presents great possibilities for clinical implementation.

$\zeta$  Potential of the dispersion was  $-36.0 \pm 1.2$  mV (at pH  $4.2 \pm 0.1$ ). At least one of the surfactants (AG) is expected to be negatively charged at this pH ( $pK_a$  of the carboxylic group on one of the glucuronic rings of glycyrrhizic acid is below 4 (Koide et al., 1997; Zeng and Hu, 2008) while SbPC has an isoelectric point of 4.15 (Spernath et al., 2007)).

The resultant  $\zeta$  potential is sufficiently high in its absolute value to provide electrostatic stabilization of the particles in the dispersion and should be attributed to surfactant adsorption onto the particle surface.  $\zeta$  Potential evaluated at normal physiological blood pH was  $-41.7 \pm 0.9$  mV. The increase may be attributed to the negative charge of both glucuronic carboxylic groups of AG at pH 7.4 ( $pK_a$  of second carboxylic group on the glucuronic ring is 4.6–4.7 (Koide et al., 1997; Zeng and Hu, 2008)) and to the domination of negative charge on SbPC molecules.

### 3.5. Control experiments

To prove these results are not due to simple solubilization of celecoxib in a micellar solution of the surfactants, the celecoxib raw material (large crystals) was dispersed in an aqueous solution of the two surfactants at concentrations similar to those in 0.5 wt% aqueous dispersion of the powder. The suspensions were incubated at various temperatures (room temperature, 40 and 60 °C) to determine the temperature effect on possible solubilization of celecoxib within micelles. The presence of solubilized celecoxib was evaluated immediately after the incubation period by the filtration experiment (without cooling the suspension), as above. It was found that at room temperature, only  $10 \pm 0.5$  wt% of the celecoxib was present in the filtrate (solubilized within the micelles of the surfactants), while at 40 °C the filtrate fraction was  $17 \pm 0.3$  wt% and at 60 °C it was  $30 \pm 3$  wt% (60 °C is the maximal temperature applied during the spray drying process). The increase in the fraction found in the filtrate with temperature elevation is probably caused by both solubility increase and solubilization enhancement. It should be emphasized that all the experiments of dispersing nanopowder in water were conducted at room temperature and resulted in much higher celecoxib concentrations, about 95 wt% of the drug.

To eliminate the possibility of formation of a solid solution, celecoxib, SbPC, and AG were dispersed in nBuAc and secBuOH and then heated to evaporate the solvents. The obtained solid mass was not easily dispersible in water and formed a turbid dispersion in which a rapid sedimentation occurred.

It can be therefore concluded that the oil-in-water microemulsion is a necessary template for the formation of water-dispersible nanoparticles.

### 3.6. Dissolution test

The effect of celecoxib nanosizing on its dissolution rate was evaluated by dissolution experiments. The dissolution profiles of the drug were measured for the nanopowder, celecoxib bulk powder, and celecoxib bulk powder in presence of surfactants (Fig. 7).

It is clear that a tremendous increase in both dissolution rate and final concentration of the celecoxib is achieved for the nanopowder within 30 min. Due to technical difficulty of assuring constant temperature during ultrafiltration, no separation was made between truly dissolved and nanometrically dispersed celecoxib in this experiment. However, dissolution test was held at higher temperature and lower celecoxib concentration than the separation experiment described in Section 3.4, thus a dissolved fraction higher than 21 wt% may be expected. Both truly dissolved and nanometrically dispersed celecoxib is expected to attain a high bioavailability level. This result demonstrates the significant advantage of celecoxib powder pre-

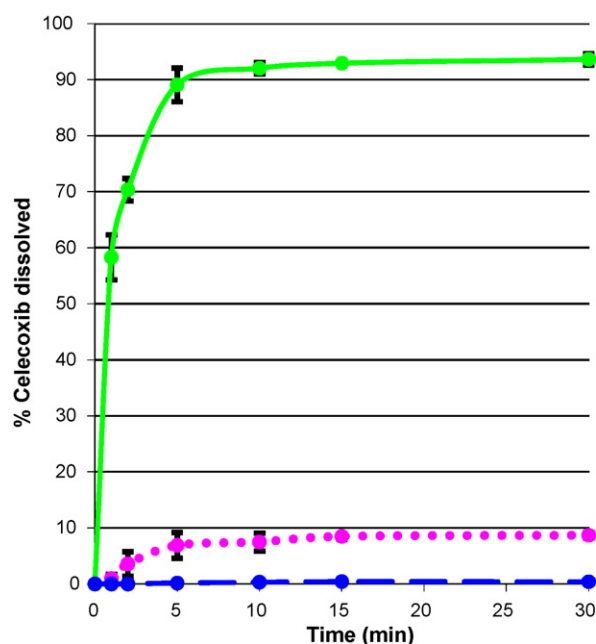


Fig. 7. Comparative dissolution test of (—) nanopowder, (---) celecoxib bulk powder, and (.....) celecoxib bulk powder in the presence of surfactants.

pared by the proposed method over the conventional particulate drug.

## 4. Summary

We demonstrate a process for obtaining nanopowder of poorly water-soluble drugs by rapid evaporation of drug-loaded volatile microemulsions, which are stabilized by natural, pharmaceutically acceptable surfactants. This method brings several advantages over commonly used nanoparticle preparation systems:

- (1) The microemulsion route is simple, does not require any special instruments or high-energy investment, and can be easily scaled-up to be utilized in the pharmaceutical industry.
- (2) Nanoparticles smaller than 100 nm can be formed since the size of the microemulsion droplets is less than a few tens of nanometers. The bioavailability of particles of such size is expected to be very high.
- (3) The final solid, dry, free-flowing nanometric powder may be easily incorporated into various drug dosage forms and stored for a long period of time.

The phase diagram of a microemulsion system containing SbPC and AG with a broad isotropic region was shown. It was found that this system is fully dilutable with water along the dilution line 4:6 (oil to surfactant ratio). This property of the microemulsion system raises a possibility for its implementation in drug delivery either as is, by using drug-loaded microemulsion that can be diluted many times in biofluids without phase separation (upon replacing the solvents with a pharmaceutically approved one), or as a template for drug nanoparticle formation.

After spray drying, a fine, solvent free powder is obtained. This powder is easily dispersible in water to form a transparent and stable dispersion of drug nanoparticles with an average particle size as small as 17 nm.

Since the resultant nanoparticles are in the form of dry powder, improved chemical and microbial stability is expected, thus prolonging the shelf-life of the preparation. Such powder may be incorporated into tablets, capsules, or other orally administered

dosage forms. Celecoxib concentration in common commercial products varies between 100 and 200 mg. By using the powder compositions described in this study, it is possible to attain the 100 mg dose without exceeding the overall tablet or capsule weight of 1 g. The experiments indicate that this powder shows an about 10-fold increase in dissolution profile compared to the particulate drug in the presence of surfactants. Based on the dissolution tests it is expected that the potency of celecoxib in nanoparticles will be increased compared to the particular drug, thus the required drug concentration in the tablet or capsule will be reduced.

It is expected that the same process will be suitable for a variety of water-insoluble drugs. In the near future, bioavailability and toxicity studies of the resultant celecoxib nanoparticles will be evaluated *in vivo*.

## Acknowledgement

The authors would like to thank Dr. Gal Goshen for performing image analysis.

## References

- Aranberri, I., Beverley, K.J., Binks, B.P., Clint, J.H., Fletcher, P.D.L., 2002. How do emulsions evaporate? *Langmuir* 18, 3471–3475.
- Archakov, A.I., Guseva, M.K., Uchaikin, V.F., Tikhonova, E.G., Ipatova, O.M., 2007. Medicinal forms of phospholipid preparations and methods for their preparation. International Patent WO/2007/020505.
- Auman, J.T., Church, R., Lee, S.Y., Watson, M.A., Fleschman, J.W., McLeod, H.L., 2008. Celecoxib pre-treatment in human colorectal adenocarcinoma patients is associated with gene expression alterations suggestive of diminished cellular proliferation. *Eur. J. Cancer* 44, 1754–1760.
- Baboota, S., Faiyaz, S., Ahuja, A., Ali, J., Shafiq, S., Ahmad, S., 2007. Development and validation of a stability-indicating HPLC method for analysis of celecoxib (CXB) in bulk drug and microemulsion formulations. *Acta Chromatogr.* 18, 116–129.
- Bellare, J.R., Davis, H.T., Scriven, L.E., Talmon, Y., 1988. Controlled environment vitrification system: an improved sample preparation technique. *J. Electron Microsc.* 10, 87–111.
- Bertagnolli, M.M., Eagle, C.J., Zaubner, A.G., Redston, M., Solomon, S.D., Kim, K., Tang, J., Rosenstein, R.B., Wittes, J., Corle, D., Hess, T.M., Woloj, G.M., Boiserie, F., Anderson, W.F., Viner, J.L., Bagheri, D., Burn, J., Chung, D.C., Dewar, T., Foley, T.R., Hoffman, N., Macrae, F., Pruitt, R.E., Saltzman, J.R., Salzberg, B., Sylwestrowicz, T., Gordon, G.B., Hawk, E.T., 2006. Celecoxib for the prevention of sporadic colorectal adenomas. *N. Engl. J. Med.* 355, 873–884.
- Bushrab, F.N., Müller, R.H., 2003. Nanocrystals of poorly soluble drugs for oral administration. *J. New Drugs* 5, 20–22.
- Chan, A.T., Zaubner, A.G., Hsu, M., Breazna, A., Hunter, D.J., Rosenstein, R.B., Eagle, C.J., Hawk, E.T., Bertagnolli, M.M., 2009. Cytochrome P450 2C9 variants influence response to celecoxib for prevention of colorectal adenoma. *Gastroenterology* 136, 2127–2136.
- Chen, J.F., Zhang, J.Y., Shen, Z.G., Zhong, J., Yun, J., 2006. Preparation and characterization of amorphous cefuroxime axetil drug nanoparticles with novel technology: high-gravity antisolvent precipitation. *Ind. Eng. Chem.* 45, 8723–8727.
- Chen, X.X., Young, T.J., Sarkari, M., Williams, R.O., Johnston, K.P., 2002. Preparation of cyclosporine A nanoparticles by evaporative precipitation into aqueous solution. *Int. J. Pharm.* 242, 3–14.
- Clint, J.H., Fletcher, P.D.L., Todorov, I.T., 1999. Evaporation rates of water from water-in-oil microemulsions. *Phys. Chem. Chem. Phys.* 1, 5005–5009.
- Cui, H., Hodgdon, T.K., Kaler, E.W., Abezgauz, L., Danino, D., Lubovsky, M., Talmon, Y., Pochan, D.J., 2007. Elucidating the assembled structure of amphiphiles in solution via cryogenic transmission electron microscopy. *Soft Matter* 3, 945–955.
- Danino, D., Bernheim-Groswasser, A., Talmon, Y., 2001. Digital cryogenic transmission electron microscopy: an advanced tool for direct imaging of complex fluids. *Colloid Surf. A* 183, 113–122.
- Dannenberg, A.J., Subbaramaiah, K., 2003. Targeting cyclooxygenase-2 in human neoplasia: rationale and promise. *Cancer Cell* 4, 431–436.
- De Gennes, P.G., Taupin, C., 1982. Microemulsions and the flexibility of oil/water interfaces. *J. Phys. Chem.* 86, 2294–2304.
- Debuigne, F., Jeuniaux, L., Wiame, M., Nagy, J.B., 2000. Synthesis of organic nanoparticles in different W/O microemulsions. *Langmuir* 16, 7605–7611.
- Desgouilles, S., Vauthier, C., Bazile, D., Vacus, J., Grossiord, J.L., Veillard, M., Couvreur, P., 2003. The design of nanoparticles obtained by solvent evaporation: a comprehensive study. *Langmuir* 19, 9504–9510.
- Destree, C., Debuigne, F., Jeuniaux, L., Nagy, J.B., 2006. Mechanism of formation of inorganic and organic nanoparticles from microemulsions. *Adv. Colloid. Interface Sci.* 123–126, 353–367.
- Destree, C., Ghijsen, J., Nagy, J.B., 2007. Preparation of organic nanoparticles using microemulsions: their potential use in transdermal delivery. *Langmuir* 23, 1965–1973.
- Detrembleur, C., De Nayer, J., Van Den Hecke, A., 2005. Celecoxib improves the efficiency of the locomotor mechanism in patients with knee osteoarthritis. A randomised, placebo, double-blind and cross-over trial. *Osteoarthr. Cartil.* 13, 206–210.
- Dhingra, D., Sharma, A., 2005. Evaluation of antidepressant-like activity of glycyrrhizin in mice. *Indian J. Pharmacol.* 37, 390–394.
- Gupta, P., Chawla, G., Bansal, A.K., 2004. Physical stability and solubility advantage from amorphous celecoxib: the role of thermodynamic quantities and molecular mobility. *Mol. Pharm.* 1, 406–413.
- Horn, D., Rieger, J., 2001. Organic nanoparticles in the aqueous phase—theory, experiment, and use. *Angew. Chem. Int. Ed.* 40, 4331–4361.
- Hu, J.H., Johnston, K.P., Williams, R.O., 2004. Rapid dissolving high potency dantrol powder produced by spray freezing into liquid process. *Int. J. Pharm.* 271, 145–154.
- Keck, C.M., Muller, R.H., 2006. Drug nanocrystals of poorly soluble drugs produced by high pressure homogenisation. *Eur. J. Pharm. Biopharm.* 62, 3–16.
- Kivitz, A.J., Espinoza, L.R., Sherrer, Y.R., Liu-Dumaw, M., West, C.R., 2007. A comparison of the efficacy and safety of celecoxib 200 mg and celecoxib 400 mg once daily in treating the signs and symptoms of psoriatic arthritis. *Semin. Arthritis Rheum.* 37, 164–173.
- Knapp, L.F., 1921. The solubility of small particles and the stability of colloids. *Trans. Faraday Soc.* 17, 457–465.
- Koide, M., Ukawa, J., Tagaki, W., Tamagaki, S., 1997. Hydrolysis of nonionic ester surfactants facilitated by potassium beta-glycyrrhizinate: implication of catalytic functions played by the carboxyl groups. *J. Am. Oil Chem. Soc.* 74, 49–54.
- Lin, A.H., Liu, Y.M., Huang, Y., Sun, J.B., Wu, Z.F., Zhang, M., Ping, Q.N., 2008. Glycyrrhizin surface-modified chitosan nanoparticles for hepatocyte-targeted delivery. *Int. J. Pharm.* 359, 247–253.
- Lu, G.W., Hawley, M., Smith, M., Geiger, B.M., Pfund, W., 2006. Characterization of a novel polymorphic form of celecoxib. *J. Pharm. Sci.* 95, 305–317.
- Magdassi, S., Netivi (Donio), H., Margulis-Goshen, K., 2007. Organic nanoparticles obtained from microemulsions by solvent evaporation. International Patent Application Number: PCT/IL2007/001136.
- Margulis-Goshen, K., Magdassi, S., 2009. Formation of simvastatin nanoparticles from microemulsion. *Nanomedicine* 5, 274–281.
- Margulis-Goshen, K., Netivi (Donio), H., Major, D.T., Gradzielski, M., Raviv, U., Magdassi, S., 2010. Formation of organic nanoparticles from volatile microemulsions. *J. Colloid Interface Sci.* 342, 283–292.
- Matteucci, M.E., Brettmann, B.K., Rogers, T.L., Elder, E.J., Williams, R.O., Johnston, K.P., 2007. Design of potent amorphous drug nanoparticles for rapid generation of highly supersaturated media. *Mol. Pharm.* 4, 782–793.
- Matteucci, M.E., Hotze, M.A., Johnston, K.P., Williams, R.O., 2006. Drug nanoparticles by antisolvent precipitation: mixing energy versus surfactant stabilization. *Langmuir* 22, 8951–8959.
- Merisko-Liversidge, E.M., Liversidge, G.G., 2008. Drug nanoparticles: formulating poorly water-soluble compounds. *Toxicol. Pathol.* 36, 43–48.
- Niwa, T., Shimabara, H., Kondo, M., Danjo, K., 2009. Design of porous microparticles with single-micron size by novel spray freeze-drying technique using four-fluid nozzle. *Int. J. Pharm.* 382, 88–97.
- Noyes, A.A., Whitney, W.R., 1897. The rate of solution of solid substances in their own solutions. *J. Am. Chem. Soc.* 19, 930–934.
- Oh, H.M., Lee, S., Park, Y.N., Choi, E.J., Choi, J.Y., Kim, J.A., Kweon, J.H., Han, W.C., Choi, S.C., Han, J.K., Son, J.K., Lee, S.H., Jun, C.D., 2009. Ammonium glycyrrhizinate protects gastric epithelial cells from hydrogen peroxide-induced cell death. *Exp. Biol. Med.* (Maywood) 234, 263–277.
- Paolino, D., Lucania, G., Mardente, D., Alhaique, F., Fresta, M., 2005. Ethosomes for skin delivery of ammonium glycyrrhizinate: in vitro percutaneous permeation through human skin and in vivo anti-inflammatory activity on human volunteers. *J. Controlled Release* 106, 99–110.
- Paulson, S.K., Vaughn, M.B., Jessen, S.M., Lawal, Y., Gresk, C.J., Yan, B., Maziasz, T.J., Cook, C.S., Karim, A., 2001. Pharmacokinetics of celecoxib after oral administration in dogs and humans: effect of food and site of absorption. *J. Pharmacol. Exp. Ther.* 297, 638–645.
- Perrut, A., Jung, J., Leboeuf, F., 2005. Enhancement of dissolution rate of poorly-soluble active ingredients by supercritical fluid processes Part I: micronization of neat particles. *Int. J. Pharm.* 288, 3–10.
- Rabinow, B.E., 2004. Nanosuspensions in drug delivery. *Nat. Rev. Drug Discov.* 3, 785–796.
- Shono, Y., Jantravid, E., Janssen, N., Kesiosoglou, F., Mao, Y., Vertzoni, M., Reppas, C., Dressman, J.B., 2009. Prediction of food effects on the absorption of celecoxib based on biorelevant dissolution testing coupled with physiologically based pharmacokinetic modeling. *Eur. J. Pharm. Biopharm.* 73, 107–114.
- Spemath, A., Aserin, A., Ziserman, L., Danino, D., Garti, N., 2007. Phosphatidylcholine embedded microemulsions: physical properties and improved Caco-2 cell permeability. *J. Controlled Release* 119, 279–290.
- Steippler, E., Kopp, S., Dressman, J.B., 2004. Comparison of US pharmacopeia simulated intestinal fluid TS (without pancreatin) and phosphate standard buffer pH 6.8, TS of the International Pharmacopeia with the respect to their use in *in vitro* dissolution testing. *Dissolut. Technol.*, 6–10.
- Trotta, M., Gallarate, M., Carloti, M.E., Morel, S., 2003. Preparation of griseofulvin nanoparticles from water-dilutable microemulsions. *Int. J. Pharm.* 254, 235–242.
- Trotta, M., Peira, E., Carloti, M.E., Gallarate, M., 2004. Deformable liposomes for dermal administration of methotrexate. *Int. J. Pharm.* 270, 119–125.
- Turk, M., Hils, P., Helfgen, B., Schaber, K., Martin, H.J., Wahl, M.A., 2002. Micronization of pharmaceutical substances by the rapid expansion of supercritical solutions (RESS): a promising method to improve bioavailability of poorly soluble pharmaceutical agents. *J. Supercrit. Fluid.* 22, 75–84.

- Yelland, M.J., Nikles, C.J., McNairn, N., Del Mar, C.B., Schluter, P.J., Brown, R.M., 2007. Celecoxib compared with sustained-release paracetamol for osteoarthritis: a series of n-of-1 trials. *Rheumatology (Oxford)* 46, 135–140.
- Yoshioka, H., Fujita, T., Goto, A., 1989. Effect of glycyrrhizin on the phosphatidylcholine water-system ESR and calorimetric study. *J. Colloid Interface Sci.* 133, 442–446.
- Zeng, C.X., Hu, Q., 2008. Determination of the polyacid dissociation constants of glycyrrhizic acid. *Indian J. Chem. A* 47, 71–74.
- Zhu, Z.X., Anacker, J.L., Ji, S.X., Hoyer, T.R., Macosko, C.W., Prud'homme, R.K., 2007. Formation of block copolymer-protected nanoparticles via reactive impingement mixing. *Langmuir* 23, 10499–10504.